

# Extremely brilliant crystal-based light sources

Gennady B. Sushko,<sup>1</sup> Andrei V. Korol,<sup>1,\*</sup> and Andrey V. Solov'yov<sup>1,†</sup>

<sup>1</sup>MBN Research Center, Altenhöferallee 3, 60438 Frankfurt am Main, Germany

Brilliance of novel gamma-ray Crystal-based Light Sources (CLS) that can be constructed through exposure of oriented crystals to beams of ultrarelativistic charged particles is calculated basing on the atomistic scale numerical modeling of the channeling process. In an exemplary case study, the brilliance of radiation emitted in a diamond-based Crystalline Undulator LS by a 10 GeV positron beam available at present at the SLAC facility is computed. Intensity of CU radiation in the photon energy range  $10^0 - 10^1$  MeV, which is inaccessible to conventional synchrotrons, undulators and XFELs, greatly exceeds that of laser-Compton scattering LSs and can be higher than predicted in the Gamma Factory proposal to CERN. Construction of novel CLSs is a challenging task which constitutes a highly interdisciplinary field entangling a broad range of correlated activities. CLSs provide a low-cost alternative to conventional LSs and have enormous number of applications.

Development of light sources (LS) operational at wavelengths  $\lambda$  well below one angstrom (corresponding photon energies  $\hbar\omega > 10$  keV) is a challenging goal of modern physics. Sub-angstrom wavelength, ultrahigh brilliance, tunable LSs will have a broad range of exciting potential cutting-edge applications. These applications include exploring elementary particles, probing nuclear structures and photonuclear physics, and examining quantum processes, which rely heavily on gamma-ray sources in the MeV to GeV range [1–3]. Modern X-ray Free-Electron-Laser (XFEL) can generate X-rays with wavelengths  $\lambda \sim 1$  Å [5–8]. Existing synchrotron facilities provide radiation of shorter wavelengths but orders of magnitude less intensive [9–11]. Therefore, to create a powerful LS in the range  $\lambda \ll 1$  Å new approaches and technologies are needed.

Several schemes for short-wavelengths LS, which do not utilize magnets, have been proposed [1–3, 17]

To be mentioned are the schemes based on the Compton scattering process in the course of which a low-energy laser photon backscatters from an ultra-relativistic electron thus acquiring increase in the energy proportional to the squared Lorentz factor  $\gamma = \varepsilon/mc^2$  [12]. This method has been used for producing gamma-rays in a broad,  $10^1$  keV –  $10^1$  MeV, energy range [13, 14]. Reviews on Compton gamma-ray beams and some of the commissioned facilities are available [3, 4, 15, 16].

The Compton scattering also occurs if the scatterer is an atomic (ionic) electron which moves being bound to a nucleus. This phenomenon is behind the Gamma Factory (GF) proposal for CERN [17, 18] that implies using a beam of ultra-relativistic ions in the backscattering process. The GF project aims at creating, storing, and exploiting relativistic beams of partly stripped high energy ( $\gamma = 30 \dots 3000$ ) atomic ions that stored in the Super Proton Synchrotron at CERN. In this scheme, a resonant excitation of an ion with the laser beam tuned to the atomic transitions frequencies is followed by the process of spontaneous emission of photons. Due to the relativistic Doppler effect, the energy of photons emitted in the direction of the beam is boosted by a factor of

up to  $4\gamma^2$  as compared to the energy of the laser light. Due to huge excess (a factor up to  $10^9$ ) of resonant photon absorption cross section compared to that of photon scattering from a free electron, the intensity of an atomic-beam-driven LS is expected to be several orders of magnitude higher than what is possible with Compton gamma-ray sources driven by an electron beam. It is planned to reach the photon flux of the order of  $10^{17}$  photons/s in the particularly interesting gamma-ray energy domain of  $1 \leq E_{\text{ph}} \leq 400$  MeV.

In recent years [1, 19] significant efforts of the research and technological communities have been devoted to design and practical realization of novel gamma-ray Crystal-based LSs (CLS) that can be set up by exposing oriented crystals to beams of ultrarelativistic positrons or electrons. Manufacturing of CLSs is a subject of the currently running European project 'N-LIGHT' [20]. In Ref. [1] brilliance of radiation emitted in the photon energy range  $10^0$ - $10^1$  MeV in a crystalline undulator (CU)-based LSs has been estimated using the model based the continuous interplanar potential concept [21] and utilizing the phenomenological approach to describe the dechanneling process.

This Letter reports on the important progress in the field providing accurate predictions for the brilliance of the CU-LS on the basis of *all-atom molecular dynamics simulations* of relativistic particles channeling and radiation in oriented crystals. The exemplary case study presented shows that using the positron beam available at present it is realistic to achieve brilliances that exceed those of the laser-Compton scattering LSs and predicted in the GF proposal.

Numerical modeling of the channeling and related phenomena beyond the continuous potential framework has been carried out by means of the multi-purpose computer package MBN EXPLORER [25–27] and a supplementary special multitask software toolkit MBN STUDIO [28]. A special module of MBN EXPLORER allows one to simulate the motion of relativistic projectiles along with dynamical simulations of the environment [26]. The uniqueness of the computation algorithm is that it ac-

counts for the interaction of projectiles with all atoms of the environment thus making it free of simplifying model assumptions. In addition, a variety of interatomic potentials implemented facilitates rigorous simulations of various media, a crystalline one in particular. Overview of the results on channeling and radiation of charged particles in oriented linear, bent and periodically bent crystals simulated by means of MBN EXPLORER and MBN STUDIO can be found in [1, 19, 22, 27].

Construction of novel gamma-ray CLSs is a challenging task involving a broad range of correlated research and technological activities. One of the key technological task concerns manufacturing of crystals of different desired geometry. High quality of the undulator material is essential for achieving strong effects in the emission spectra. A systematic review of different technologies exploited for manufacturing of crystals of different type, geometry, size, quality, etc. one finds in Refs. [1, 19]. A brief summary is presented in Supplemental Material (SM). In this connection it is important to mention that the parameters of the periodically bent crystal (discussed below) that have been used in the simulations are accessible by means of existing modern technologies.

The model approach developed in Ref. [1] has allowed one to establish optimal parameters of a periodically bent crystal (these include crystal thickness  $L$  in the direction of beam, bending amplitude  $a$  and period  $\lambda_u$ ) that ensure the highest values of brilliance of the CU-LS for a positron beam of given energy  $\varepsilon$ , transverse beam sizes  $\sigma_{x,y}$  and angular divergence  $\sigma_{\phi_{x,y}}$ .

The current simulations have been performed for a  $\varepsilon = 10$  GeV ( $\gamma = 1.96 \times 10^4$ ) positron beam propagating through an oriented periodically bent diamond (110) single crystal. The following values of the beam sizes and divergence were used:  $\sigma_{x,y} = 32, 10$  microns and  $\sigma_{\phi_{x,y}} = 10, 30$   $\mu$ rad, respectively. These values correspond to normalized emittance  $\gamma\epsilon_{x,y} = \gamma\sigma_{\phi_{x,y}}\sigma_{x,y} = 6.3, 5.9$  m- $\mu$ rad and are within the ranges indicated for the FACET-II beam (before longitudinal compression) available at the SLAC facility, see Table 4.6 in Ref. [23]. The peak current of the beam is  $I_{\text{peak}} = 3.1$  kA.

The simulations have been performed using the following values of bending amplitude and period:  $a = 21$  Å and  $\lambda_u = 85$  microns. These quantities result in the peak energy  $\hbar\omega_0 = 2$  MeV of the CU radiation emitted in the forward direction. The frequency  $\omega_0$  of fundamental harmonic of the CU radiation reads

$$\omega_0 = \frac{2\gamma^2\Omega_u}{1 + K^2/2} \quad (1)$$

where  $K = 2\pi\gamma a/\lambda_u$  stands for the so-called undulator parameter and  $\Omega_u = 2\pi c/\lambda_u$ .

Within the framework of the model approach [1] it was found that for the quoted values of  $\varepsilon$ ,  $\sigma_{x,y}$ ,  $\sigma_{\phi_{x,y}}$ ,  $a$  and  $\lambda_u$  the brilliance of the CU-LS at 2 MeV reaches its maximum value for crystal thickness  $L$  that accom-

modates  $N_u = 83$  undulator periods along the incident beam direction (the  $z$ -axis). The current simulations have been performed for several values of  $L$  within the range  $L \leq 85 \times 85 = 7055$  microns.

To simulate the trajectories of the beam particles in the crystalline medium, the  $y$ -axis was chosen along the  $\langle 110 \rangle$  axial direction. This choice ensures that a sufficiently big fraction  $\xi$  of the incident beam is accepted in the channeling mode at the crystal entrance. For a Gaussian beam this fraction can be estimated as  $\xi = (2\pi\sigma_{\phi_y}^2)^{-1/2} \int_{-\Theta_L}^{\Theta_L} \exp(-\phi^2/2\sigma_{\phi_y}^2) d\phi$  where  $\Theta_L$  stands for Lindhard's critical angle. Using  $U_0 \approx 20$  eV for the interplanar potential depth in diamond(110) one calculates  $\Theta_L = (2U_0/\varepsilon)^{1/2} \approx 63$   $\mu$ rad that exceeds by a factor of two the divergence  $\phi_y = 30$   $\mu$ rad. The beam divergence  $\phi_x = 10$   $\mu$ rad along the  $x$  transverse direction is much smaller than the natural emission angle  $\theta_\gamma = \gamma^{-1} \approx 50$   $\mu$ rad. As a result, one can expect that big fraction of radiation emitted by the channeling particles will be collected within the cone  $\theta_0 \leq \theta_\gamma$  centered along the incident beam.

The simulations performed aimed at providing accurate quantitative data on the brilliance of a CU-LS. Brilliance,  $B$ , of a LS is proportional to the number of photons  $\Delta N_\omega$  of frequency within the interval  $[\omega - \Delta\omega/2, \omega + \Delta\omega/2]$  emitted in the cone  $\Delta\Omega$  per unit time interval, unit source area, unit solid angle and per a bandwidth (BW)  $\Delta\omega/\omega$  [29]. To calculate this quantity it is necessary to know the beam electric current  $I$ , its transverse sizes and divergences as well as the divergence angle  $\phi = \sqrt{\Delta\Omega/2\pi}$  and the 'size'  $\sigma = \lambda/4\pi\phi$  of the photon beam. Explicit expression for  $B$  reads [30]

$$B_\omega = \frac{\Delta N_\omega}{10^3 (\Delta\omega/\omega) (2\pi)^2 E_x E_y} \frac{I}{e}, \quad (2)$$

Here  $I$  is the electric current (in amperes) of the beam of particles,  $e$  is the elementary charge. The quantities  $E_{x,y} = (\sigma^2 + \sigma_{x,y}^2)^{1/2} (\phi^2 + \sigma_{\phi_{x,y}}^2)^{1/2}$  stand for the total emittance of the photon source in the transverse directions. Commonly, brilliance is measured in [photons/s/mrad<sup>2</sup>/mm<sup>2</sup>/0.1% BW]. To achieve this in (2) one substitutes  $I$  in amperes,  $\sigma$ ,  $\sigma_{x,y}$  in millimeters, and  $\phi$ ,  $\sigma_{\phi_{x,y}}$  in milliradians. If one uses the peak value of the current,  $I_{\text{peak}}$ , then the corresponding quantity is called *peak brilliance*,  $B_{\text{peak}}$ .

The number of photons within the BW is proportional to the spectral distribution  $dE(\theta \leq \theta_0)/d(\hbar\omega)$  of the energy radiated per particle in the solid angle  $\Delta\Omega \approx 2\pi\theta_0^2/2$  (the emission cone  $\theta_0$  is assumed to be small,  $\theta_0 \ll 1$ ):  $\Delta N_\omega = (dE(\theta \leq \theta_0)/d(\hbar\omega)) \Delta\omega/\omega$ . Using this relation one writes the brilliance in terms of the spectral distribution:

$$B_\omega = \frac{dE(\theta \leq \theta_0)}{d(\hbar\omega)} \frac{1.58 \times 10^{14} I}{E_x E_y}. \quad (3)$$

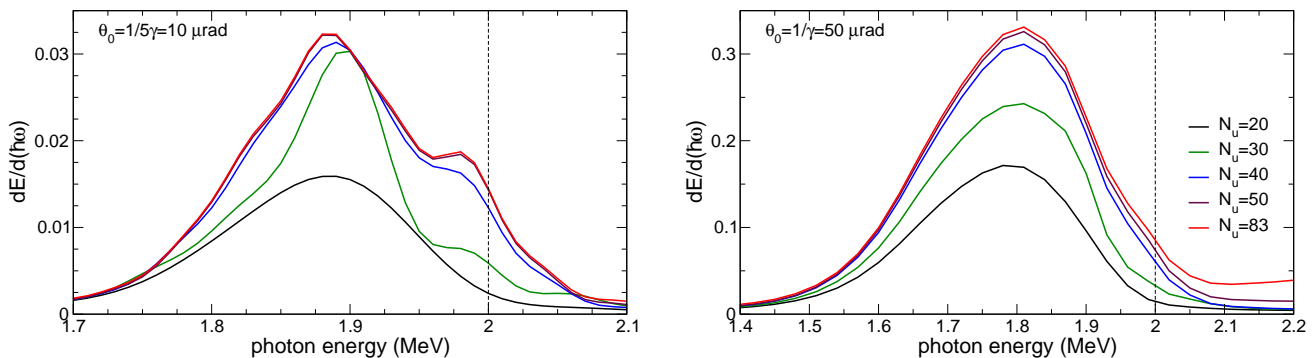


FIG. 1. Spectral distribution  $dE(\theta \leq \theta_0)/d(\hbar\omega)$  emitted within the cones  $\theta_0 = (5\gamma)^{-1} = 10 \mu\text{rad}$  (left panel) and  $\gamma^{-1} = 50 \mu\text{rad}$  (right panel) corresponding to different number of undulator periods  $N_u$  as indicated in the common legend in the right panel. In both panels, a dashed line marks the value  $\hbar\omega_0 = 2 \text{ MeV}$  which is the the position of the on-axis first harmonic peak as follows from Eq. (1)

In the simulations, the spectral distribution  $dE_j(\theta \leq \theta_0)/d(\hbar\omega)$  has been calculated for each trajectory simulated ( $j = 1, \dots, N_0$  with the total number of trajectories  $N_0 \approx 3 \times 10^3$ ). Initial conditions at the crystal entrance (the transverse coordinates and velocities) have been generated using the normal distributions with the deviations  $\sigma_{x,y}$  and  $\sigma_{\phi_{x,y}}$  quoted above. The resulting spectral distribution used to calculate the brilliance (3) has been obtained by averaging the individual spectra:  $dE(\theta \leq \theta_0)/d(\hbar\omega) = N_0^{-1} \sum_j dE_j(\theta \leq \theta_0)/d(\hbar\omega)$ . The sum is carried out over all simulated trajectories, and thus, it takes into account the contribution of the channeling segments as well as of those corresponding to the non-channeling regime. More details on the simulation procedure as well on the formalism behind it one finds in the review paper [19].

In what follows the emission of radiation from the diamond(110)-based CU undulator is discussed within the photon energy range  $\hbar\omega = 1 - 2.5 \text{ MeV}$ , which contains the first harmonic energy estimated from Eq. (1).

Figure 1 presents the spectral distribution of radiation emitted within the narrow cone  $\theta_0 = (5\gamma)^{-1} = 10 \mu\text{rad}$  (left graph) and the wider one  $\theta_0 = \gamma^{-1} = 50 \mu\text{rad}$  (right graph). The calculations were performed for different number of undulator periods,  $N_u$ , as indicated in the common legend shown in the right graph.

Several features of the computed spectra are to be noted. First, all peaks are red-shifted from the estimate  $\hbar\omega_0 = 2 \text{ MeV}$  that follows from Eq. (1). The shift increases with the emission cone. Second, for large number of periods the spectrum becomes virtually independent on the crystal length: in both panels all spectra become very close for  $N_u \gtrsim 50$ .

To provide an explanation to both of these features we first note that in the vicinity of maximum the emission spectrum is mainly formed by the particles, which move in the channeling mode through the whole crystal (see Figure S2 in SM). Therefore, the evolution of the

spectrum is related, to a great extent, to the dynamics of *channeling* particles in the course of their propagation through the crystalline medium. Eq. (1) describes accurately the on-axis frequency of the fundamental harmonic in an ideal planar undulator, in which a particle moves along a perfect cosine trajectory  $y(z) = a \cos(2\pi z/\lambda_u)$ . In a CU, a channeling particle experiences (i) channeling oscillations while moving along a periodically bent centerline, and (ii) stochastic motion along the  $x$  axis due to the multiple scattering from crystal constituents. The channeling oscillations lead to the following modification of the undulator parameter:  $K^2 \rightarrow K^2 + K_{\text{ch}}^2$  [31]. Here  $K_{\text{ch}} \propto 2\pi\gamma a_{\text{ch}}/\lambda_{\text{ch}}$  with  $a_{\text{ch}} \leq d/2$  and  $\lambda_{\text{ch}}$  being the amplitude and period of the channeling oscillations. In the case of positron channeling, assuming harmonicity of the oscillations, one carries out averaging over the allowed values of  $a_{\text{ch}}$  and finds  $\langle K_{\text{ch}}^2 \rangle = 2\gamma U_0/3mc^2$  [22]. For  $\varepsilon = 10 \text{ GeV}$  in diamond(110) ( $U_0 \approx 20 \text{ eV}$ ) this results in  $\langle K_{\text{ch}}^2 \rangle \approx 0.56$ . The stochastic motion along the  $x$  axis results in a gradual increase in the rms scattering angle  $\langle \theta_x^2 \rangle$  with the penetration distance  $z$ . Hence, the motion of the particle is not restricted to the  $(yz)$  plane and its emission within the cone centered along the incident beam direction becomes off-axis. As a result, the denominator of the fraction in (1) increases,  $1 + K^2/2 \rightarrow 1 + K^2/2 + \langle K_{\text{ch}}^2 \rangle/2 + \gamma^2 \langle \theta_x^2 \rangle(z) + \gamma^2 \sigma_{\phi_x}^2$ , leading to the decrease in the fundamental harmonic frequency. The increase in the rms scattering angle leads to the saturation of the emission spectrum with the crystal thickness. Indeed, taking into account that an ultra-relativistic particle radiates, predominantly, within the cone  $1/\gamma$  along its instant velocity, the emission within the cone  $\theta_0$  along the  $z$  axis becomes negligibly small at the penetration distances  $\tilde{z}$  when the relation  $\left( \langle \theta_x^2 \rangle(\tilde{z}) + \sigma_{\phi_x}^2 \right)^{1/2} - \gamma^{-1} \gtrsim \theta_0$  becomes valid. Here the term  $\sigma_{\phi_x}^2$  accounts for the beam divergence at the crystal entrance. The spectrum saturates at  $L \sim \tilde{z}$ .

The increase in the multiple scattering angle is also the

main reason for a suppression (by a factor of  $\approx 20$  for the small aperture) of the simulated intensity as compared to the ideal undulator, see Fig. S3 in SM.

The CU radiation spectra calculated for different emission cones,  $\gamma\theta_0 = 0.1 - 4$ , are presented in the left graph of Fig. 2. All curves correspond to the crystal length  $L = 5.1$  mm ( $N_u = 60$ ). These data supplemented with the aforementioned values for the beam size, divergence and peak current allow one to calculate the peak brilliance of the CU-LS, Eq. (3). The results of calculations are shown in Fig. 2<sub>right</sub> together with the estimate (marked with filled red circle) of  $1.76 \times 10^{24}$  photons/s/mrad<sup>2</sup>mm<sup>2</sup>/0.1% BW at  $\hbar\omega = 2$  MeV obtained in Ref. [1] by within the framework of the model approach. It is seen that in contrast to  $dE(\theta \leq \theta_0)/d(\hbar\omega)$ , which is an increasing function of the emission cone, the peak brilliance is a non-monotonous function due to the presence of the terms proportional to  $\theta_0$  in the total emittance  $E_{x,y}$  that enter the denominators in Eqs. (2) and (3). In the case study considered here the maximum value  $B_{\text{peak}}^{\text{max}} \approx 3.5 \times 10^{23}$  photons/s/mrad<sup>2</sup>mm<sup>2</sup>/0.1% BW is achieved at  $\hbar\omega = 1.85$  MeV for the emission cone  $\theta_0 = 0.7/\gamma = 35 \mu\text{rad}$ . Due to the reasons discussed above the maximum is red-shifted and less intensive (approx. 5 times less) as compared to the model prediction.

The product  $\Delta N_\omega I/e$  on the right-hand side of Eq. (1) defines the number of photons per unit time interval (intensity) emitted by all particles of the beam in the cone  $\Delta\Omega$  and frequency interval  $\Delta\omega$ . Using the peak current  $I_{\text{peak}} = 3.1$  kA one calculates the peak intensity achievable in the CU with given bending parameters exposed to the FACET-II beam. Fig. 3 shows the corresponding dependences calculated for for the BW  $\Delta\omega/\omega = 0.01$  and for several emission cones as indicated. To be noted is that for the bending amplitude and period considered here the intensity of the CU radiation in the vicinity of its first harmonic exceeds the the value predicted in the GF proposal (marked with the horizontal dash-dotted line). The excess increases with the emission angle reaching the level of nearly three orders for  $\theta_0 = 1/\gamma = 50 \mu\text{rad}$ .

The results of accurate numerical simulations presented in Letter refer to the specific case study of the radiation emission by a 10 GeV positron beam (with the transverse size and divergence indicated in Ref. [23]) channeling in an oriented diamond (110) single crystal bent periodically with the amplitude  $a = 21$  Å and period  $\lambda_u = 85$  microns. These parameters maximize the peak brilliance of radiation in the vicinity of  $\hbar\omega = 2$  MeV as it has been estimated by means of the model approach developed previously [1]. The simulations demonstrated that the peak brilliance of the CU-LS is comparable to or even higher than that achievable in conventional synchrotrons in the much lower photon energy range (see also Fig. S3 in SM). The intensity of radiation greatly exceeds the values predicted in the GF proposal for CERN.

By tuning the bending amplitude and period one can maximize brilliance for given parameters of a positron beam and/or chosen type of a crystalline medium. As a result extremely high values of brilliance can be achieved in the photon energy range  $10^1 \dots 10^2$  MeV by currently available (or planned to be available in near future) positron beams [1]. For each set of the input parameters (beam energy and emittance, bending amplitude and period, crystal type and thickness, detector aperture etc.) to provide accurate data on the brilliance from a CLS rigorous numerical simulations, similar to those presented in this Letter, must be carried out. When doing this, the results of the model approach can be used as the initial estimates of the the ranges of the parameters to be used in the simulations.

It is worth mentioning that the size and the cost of CLSs are orders of magnitude less than those of modern LSs based on the permanent magnets. This opens many practical possibilities for the efficient generation of gamma-rays with various intensities and in various ranges of wavelength by means of the CLSs on the existing and newly constructed beam-lines.

The work was supported in part by the DFG Grant (Project No. 413220201) and by the H2020 RISE-ENLIGHT project (GA 872196). We acknowledge the Frankfurt Center for Scientific Computing (CSC) for providing computer facilities.

---

\* korol@mbnexplorer.com; On leave from: St. Petersburg State Marine Technical University, Leninsky ave. 101, 198262 St. Petersburg, Russia

† solovyov@mbnresearch.com; On leave from: Ioffe Physical-Technical Institute, Politekhnicheskaya 26, 194021 St. Petersburg, Russia

- [1] A. V. Korol and A. V. Solov'yov. Crystal-based intensive gamma-ray light sources. *Europ. Phys. J. D* **74**, 201 (2020).
- [2] Xing-Long Zhu, Min Chen, Su-Ming Weng, Tong-Pu Yu, Wei-Min Wang, Feng He, Zheng-Ming Sheng, Paul McKenna, Dino A. Jaroszynski, and Jie Zhang. Extremely brilliant GeV  $\gamma$ -rays from a two-stage laser-plasma accelerator. *Science Advances* **6**, eaaz7240 (2020).
- [3] C. R. Howell, M.W. Ahmed, A. Afanasev, D. Alesini, J. R. M. Annand, et al. International Workshop on Next Generation Gamma-Ray Source. arXiv preprint arXiv:2012.10843 (2020).
- [4] Y.K. Wu, N.A. Vinokurov, S. Mikhailov, J. Li, and V. Popov: High-Gain Lasing and Polarization Switch with a Distributed Optical-Klystron Free-Electron Laser. *Phys. Rev. Lett.* **96**, 224801 (2006).
- [5] A. Doerr. The new XFELs. *Nature Meth.* **13**, 33 (2018).
- [6] E. A. Seddon, J. A. Clarke, D. J. Dunning, C. Masciovecchio, C. J. Milne, F. Parmigiani, D. Rugg, J. C. H. Spence, N. R. Thompson, K. Ueda, S. M. Vinko, J. S. Wark, and E. Wurth. Short-wavelength free-electron laser sources and science: a review. *Rep. Prog. Phys.* **80**,

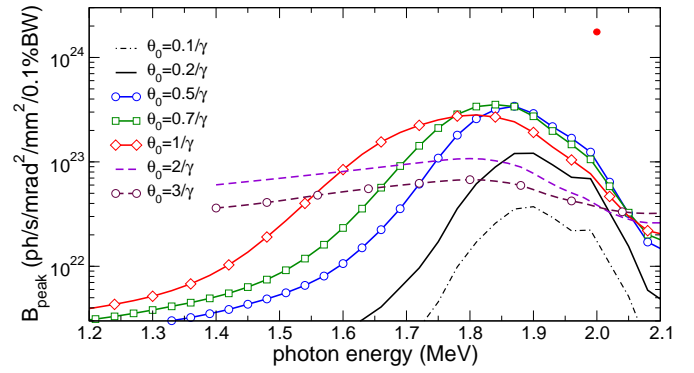
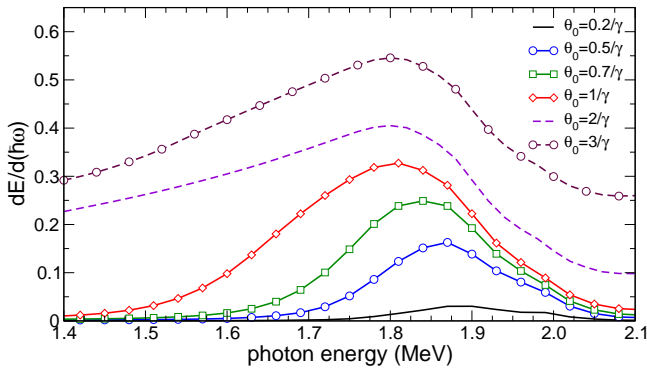


FIG. 2. *Left*: Spectral distribution  $dE(\theta \leq \theta_0)/d(\hbar\omega)$  of radiation emitted within different cones  $\theta_0$ . *Right*: Peak brilliance of CU-LS calculated for different emission cones as indicated. Red circle at  $\hbar\omega = 2$  MeV marks the result of the model approach [1]. Both panels refer to the crystal thickness  $L = 5.1$  mm ( $N_u = 60$ ).

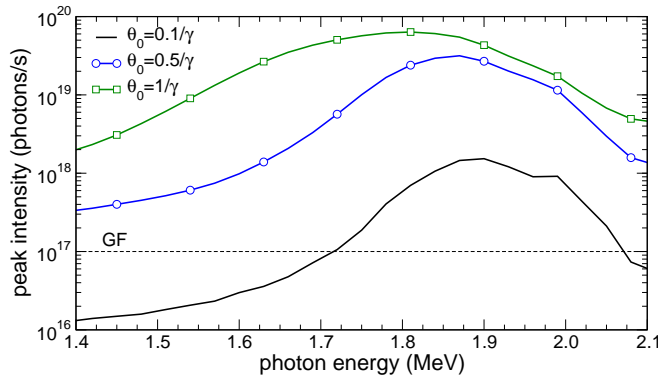


FIG. 3. Peak intensity (number of photons per second) of the diamond(110)-based CU with  $N_u = 60$  periods. Dashed line indicates the intensity  $10^{17}$  photon/s indicated in the Gamma Factory (GF) proposal for CERN [17].

- 115901 (2017).
- [7] Ch. J. Milne, Th. Schietinger, M. Aiba, A. Alarcon, J. Alex, et al. SwissFEL: The Swiss X-ray free electron laser. *Appl. Sci.* **7**, 720 (2017).
- [8] Ch. Bostedt, S. Boutet, D. M. Fritz, Z. Huang, H. J. Lee, H. T. Lemke, A. Robert, W. F. Schlotter, J. J. Turner, G. J. Williams. Linac coherent light source: The first five years. *Rev. Mod. Phys.* **88**, 015007 (2016).
- [9] M.E. Couprie. New generation of light sources: Present and future. *J. Electr. Spectrosc. Rel. Phenom.* **196**, 3 (2014).
- [10] P. F. Tavares, S. C. Leemann, M. Sjöström, and Å. Andersson. The MAX IV storage ring project. *J. Synchrotron Rad.* **21**, 862 (2014).
- [11] M. Yabashi and H. Tanaka. The next ten years of X-ray science. *Nat. Photonics* **11**, 12 (2017).
- [12] L. Federici, G. Giordano, G. Matone, G. Pasquariello, P.G. Picozza, R. Caloi, L. Casano, M.P. de Pascale, M. Mattioli, and E. Poldi. Backward Compton scattering of laser light against high-energy electrons: The LADON photon beam at Frascati. *Nuovo Cimento* **59B**, 247 (1980).
- [13] Haseeb ur Rehman, Jiyoung Lee, and Yonghee Kim. Optimization of the laser-Compton scattering spectrum for the transmutation of high-toxicity and long-living nuclear waste. *Ann. Nucl. Energy* **105**, 150 (2017).
- [14] J. M. Krämer, A. Jochmann, M. Budde, M. Bussmann, J. P. Couperus et al. Making spectral shape measurements in inverse Compton scattering a tool for advanced diagnostic applications. *Scie. Reports* **8**, 139 (2018).
- [15] G.A. Krafft and G. Priebe. Compton sources of electromagnetic radiation. *Rev. Accelerator Sci. Technol.* **3**, 147 (2010).
- [16] Norihiro Sei, Hiroshi Ogawa, and QiKa Jia. Multiple-Collision Free-Electron Laser Compton Backscattering for a High-Yield Gamma-Ray Source. *Appl. Sci.* **10**, 1418 (2020).
- [17] M. Krasny. The Gamma Factory proposal for CERN. *CERN Proc.* **1**, 249 (2018).
- [18] M. W. Krasny, A. Martens, and Y. Dutheil. Gamma factory proof-of-principle experiment: Letter of intent. *CERN-SPSC-2019-031/SPSC-I-253*, 25/09/2019 (<http://cds.cern.ch/record/2690736/files/SPSC-I-253.pdf>).
- [19] A. V. Korol and A. V. Solov'yov. All-atom relativistic molecular dynamics simulations of channeling and radiation processes in oriented crystals. *Europ. Phys. J. D* **75**, 207 (2021).
- [20] <http://www.mbnresearch.com/N-Light/main>
- [21] J. Lindhard. Influence of crystal lattice on motion of energetic charged particles. *K. Dan. Vidensk. Selsk. Mat. Fys. Medd.* **34**, 1–64 (1965)
- [22] A. V. Korol, A. V. Solov'yov, and W. Greiner, *Channeling and Radiation in Periodically Bent Crystals*, Second ed., Springer-Verlag, Berlin, Heidelberg, 2014.
- [23] SLAC Site Office: *Preliminary Conceptual Design Report for the FACET-II Project at SLAC National Accelerator Laboratory*. Report SLAC-R-1067, SLAC (2015).
- [24] H. Backe. Electron channeling experiments with bent silicon single crystals – a reanalysis based on a modified Fokker-Planck equation. *JINST* **13**, C02046 (2018).
- [25] I. A. Solov'yov, A. V. Yakubovich, P. V. Nikolaev, I. Volkovets, and A. V. Solov'yov. MesoBioNano Explorer – A universal program for multiscale computer simulations of complex molecular structure and dynamics.. *J. Comp. Phys.* **33**, 2412 (2012).
- [26] G. B. Sushko, V. G. Bezchastnov, I. A. Solov'yov, A. V. Korol, W. Greiner, and A. V. Solov'yov, Simulation of ultra-relativistic electrons and positrons channeling in

- crystals with MBN Explorer. *J. Comp. Phys.* **252**, 404 (2013).
- [27] I. A. Solov'yov, A. V. Korol, and A. V. Solov'yov, *Multi-scale Modeling of Complex Molecular Structure and Dynamics with MBN Explorer*. Springer International Publishing, Cham, Switzerland (2017).
- [28] G. B. Sushko, I. A. Solov'yov, and A. V. Solov'yov, Modeling MesoBioNano systems with MBN Studio made easy. *J. Mol. Graph. Model.* **88**, 247 (2019).
- [29] Schmüser, P., Dohlus, M. and Rossbach, J. *Ultra-violet and Soft X-Ray Free-Electron Lasers*. Springer, Berlin/Heidelberg (2008).
- [30] Kim, K.-J. Characteristics of synchrotron radiation. In: X-ray Data Booklet, pp. 2.1–2.16. Lawrence Berkeley Laboratory, Berkley (2009). (<http://xdb.lbl.gov/xdb-new.pdf>)
- [31] A.V. Korol, A. V. Solov'yov, and W. Greiner The influence of the dechanneling process on the photon emission by an ultra-relativistic positron channeling in a periodically bent crystal. *J. Phys. G* **27**, 95-125 (2001).

# Supplemental Material for "Extremely brilliant crystal-based light sources"

Gennady B. Sushko,<sup>1,\*</sup> Andrei V. Korol,<sup>1,†</sup> and Andrey V. Solov'yov<sup>1,‡</sup>

<sup>1</sup>*MBN Research Center, Altenhöferallee 3,  
60438 Frankfurt am Main, Germany*

## Abstract

In what follows some explanatory material, additional to the main text, is presented.

## METHODS FOR MANUFACTURING OF BENT CRYSTALS

Approaches that have been utilised to produce bent crystals include mechanical scratching [1], laser ablation technique [2], grooving method [3, 4], tensile/compressive strips deposition [3, 5, 6], ion implantation [7]. The most recent techniques proposed are based on sandblasting one of the major sides of a crystal to produce an amorphized layer capable of keeping the sample bent [8] and on pulsed laser melting processing that produces localized and high-quality stressing alloys on the crystal surface [9].

To increase the bending curvature one can rely on production of graded composition strained layers in an epitaxially grown  $\text{Si}_{1-x}\text{Ge}_x$  superlattice [10, 11]. Both silicon and germanium crystals have the diamond structure with close lattice constants. Replacement of a fraction of Si atoms with Ge atoms leads to bending crystalline directions. By means of this method sets of periodically bent crystals have been produced and used in channeling experiments [12]. A similar effect can be achieved by graded doping during synthesis to produce diamond superlattice [13]. Both boron and nitrogen are soluble in diamond, however, higher concentrations of boron can be achieved before extended defects appear [13, 14]. The advantage of a diamond crystal is radiation hardness allowing it to maintain the lattice integrity in the environment of very intensive beams [15].

## ADDITIONAL SIMULATED ANGULAR DISTRIBUTIONS

The data presented in this section refer to a specific case study of the radiation emission by a 10 GeV positron beam with the transverse normalized emittance  $\gamma\epsilon_x, \gamma\epsilon_y = 6.3$  and  $5.9 \text{ m-}\mu\text{rad}$ , respectively [16, 17], channeling in an oriented diamond (110) single crystal bent periodically with the amplitude  $a = 21 \text{ \AA}$  and period  $\lambda_u = 85 \text{ microns}$ . By means of the model approach developed in Ref. [18] it has been established that these parameters maximize the peak brilliance of radiation in the vicinity of  $\hbar\omega = 2 \text{ MeV}$ , which is the estimated value of the first harmonics of the crystalline undulator radiation.

Figure S1 compares the contribution of the channeling trajectories (dashed lines) to the total emission spectrum (solid lines). The curves presented corresponds to different number of the undulator  $N_u$  period as indicated. All spectra refer to the emission cone  $\theta_0 = \gamma^{-1} = 50 \mu\text{rad}$ .

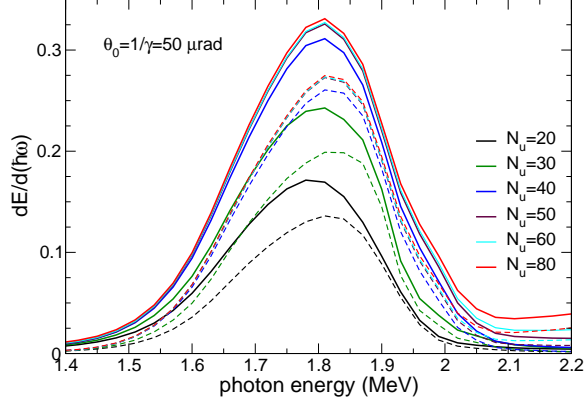


FIG. S1. Spectral distribution  $E(\theta \leq \theta_0)/(\hbar\omega)$  emitted within the cone  $\theta_0 = 50 \mu\text{rad}$  computed for different number of undulator periods  $N_u$  as indicated. Solid lines show the total emission spectra averaged over all simulated trajectories. Dashed lines represent the from those particles only that move in the channeling mode through the whole crystal.

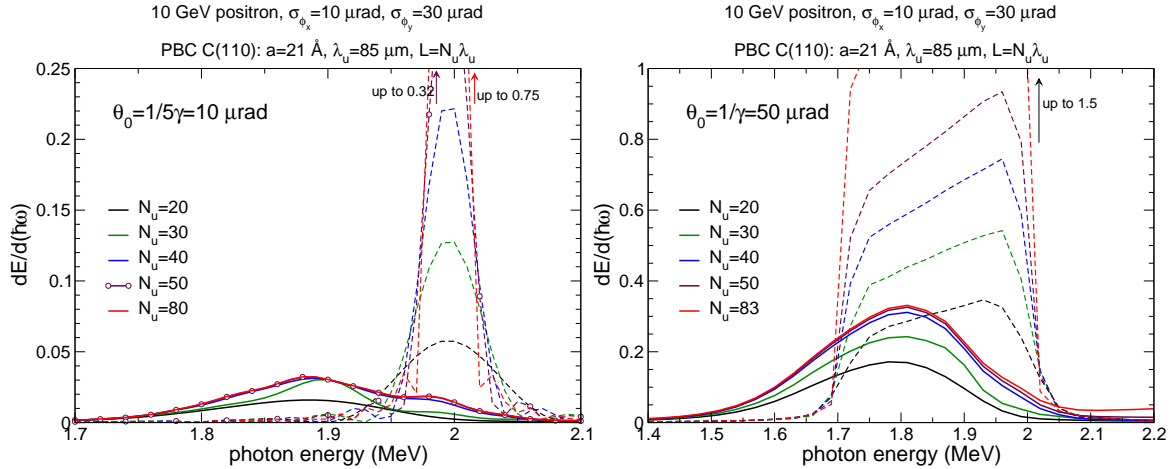


FIG. S2. Spectral distribution  $E(\theta \leq \theta_0)/(\hbar\omega)$  emitted within the cones  $\theta_0 = (5\gamma)^{-1} = 10 \mu\text{rad}$  (left panel) and  $\gamma^{-1} = 50 \mu\text{rad}$  (right panel) corresponding to different number of undulator periods  $N_u$  as indicated. Solid lines – results of numerical simulation, dashed lines correspond to ideal planar undulator.

Figure S2 compares the simulated spectral distribution of radiation (solid curves) emitted within the cones  $\theta_0 = (5\gamma)^{-1} = 10 \mu\text{rad}$  (left panel) and  $\theta_0 = \gamma^{-1} = 50 \mu\text{rad}$  (right panel) with the corresponding dependences (dashed lines) obtained for the ideal planar undulator where a projectile moves along perfect cosine trajectory  $y(z) = a \cos(2\pi z/\lambda_u)$  with  $a = 21 \text{ \AA}$ ,  $\lambda_u = 85 \text{ microns}$ . The calculations were performed for different number of undulator

periods,  $N_u$ , as indicated in the legend.

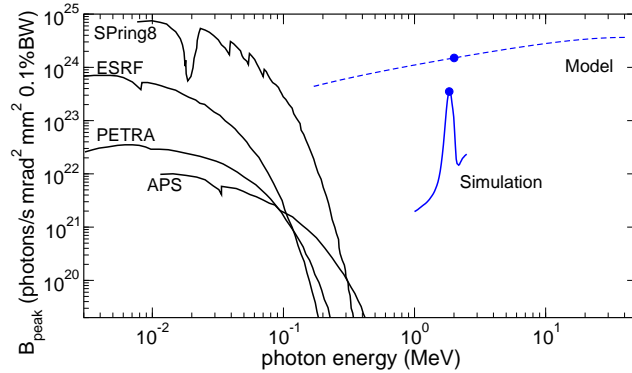


FIG. S3. Comparison of the peak brilliance available at several synchrotron radiation facilities (APS, ESRF, PETRA, SPring8) with that for the diamond(110)-based CU-LS for the FACET-II positron beam. The dashed line stands for the model estimation [18]. Solid red line - current simulations. See also explanation in the text. main text.

Figure S3 compares peak brilliance  $B_{\text{peak}}(\omega)$  of several operational synchrotron radiation facilities with that achievable by means of the diamond-based CU exposed to the FACET-II positron beam. The dashed line shows the results of the model calculations [18] that have provided, for each photon energy  $\hbar\omega$ , the highest value of  $B_{\text{peak}}(\omega)$  by scanning through the ranges of bending amplitude  $a$  and period  $\lambda_u$ . The filled circle marks the  $B_{\text{peak}}(\omega)$  value at  $\hbar\omega = 2$  MeV that corresponds to  $a = 21$  Å,  $\lambda_u = 85$  microns.

The curve labelled "Simulated" stands for the results of the current simulations. The maximum of this curve (and its position) is to be compared with the model calculation.

---

\* sushko@mbnexplorer.com

† korol@mbnexplorer.com; On leave from: St. Petersburg State Marine Technical University, Leninsky ave. 101, 198262 St. Petersburg, Russia

‡ solovyov@mbnresearch.com; On leave from: Ioffe Physical-Technical Institute, Politekhnikheskaya 26, 194021 St. Petersburg, Russia

[1] S. Bellucci, S. Bini, V. M. Biryukov, Yu. A. Chesnokov, et al. *Experimental study for the feasibility of a crystalline undulator*. Phys. Rev. Lett. **90**, 034801 (2003).

[2] P. Balling, J. Esberg, K. Kirsebom, D. Q. S. Le, U. I. Uggerhøj, S. H. Connell, J. Härtwig,

- F. Masiello, and A. Rommeveaux. *Bending diamonds by femto-second laser ablation*. Nucl. Instrum Meth. B **267**, 2952 (2009).
- [3] V. Guidi, A. Antonioni, S. Baricordi, F. Logallo, C. Malagù, E. Milan, A. Ronzoni, M. Stefancich, G. Martinelli, and A. Vomiero. *Tailoring of silicon crystals for relativistic-particle channeling*. Nucl. Instrum. Meth. B **234**, 40 (2005).
- [4] E. Bagli, L. Bandiera, V. Bellucci, A. Berra, R. Camattari, D. De Salvador, G. Germogli, V. Guidi, L. Lanzoni, D. Lietti, A. Mazzolari, M. Prest, V. V. Tikhomirov, and E. Valla. *Experimental evidence of planar channeling in a periodically bent crystal*. Eur. Phys. J. C **74**, 3114 (2014).
- [5] V. Guidi, A. Mazzolari, G. Martinelli, and A. Tralli. *Design of a crystalline undulator based on patterning by tensile  $Si_3N_4$  strips on a Si crystal*. Appl. Phys. Lett. **90**, 114107 (2007).
- [6] V. Guidi, L. Lanzoni, and A. Mazzolari. *Patterning and modeling of mechanically bent silicon plates deformed through coactive stresses*. Thin Solid Films **520**, 1074 (2011).
- [7] V. Bellucci, R. Camattari, V. Guidi, A. Mazzolari, G. Paterno, G. Mattei, C., Scian, and L. Lanzoni. *Ion implantation for manufacturing bent and periodically bent crystals*. Appl. Phys. Lett. **107**, 064102 (2015).
- [8] R. Camattari, G. Paternò, M. Romagnoni, V. Bellucci, A. Mazzolari and V. Guidi. *Homogeneous self-standing curved monocrystals, obtained using sandblasting, to be used as manipulators of hard X-rays and charged particle beams*. J. Appl. Cryst. **50** (2017) 145-151.
- [9] F. Cristiano, M. Shayesteh, R. Duffy, K. Huet, F. Mazzamuto, Y. Qiu, M. Quillec, H. H. Henrichsen, P. F. Nielsen, D. H. Petersen, A. La Magna, G. Caruso, and S. Boninelli. *Defect evolution and dopant activation in laser annealed Si and Ge*. Mat. Scie. in Semicond. Process. **42** (2016) 188-195
- [10] S. A. Bogacz and J. B. Ketterson. *Possibility of obtaining coherent radiation from a solid state undulator*. J. Appl. Phys. **60**, 177 (1986).
- [11] U. Mikkelsen and E. Uggerhøj. *A crystalline undulator based on graded composition strained layers in a superlattice*. Nucl. Instrum. Meth. B **160**, 435 (2000).
- [12] H. Backe, D. Krambrich, W. Lauth, K. K. Andersen, J. L. Hansen, and U. I. Uggerhøj. *Radiation emission at channeling of electrons in a strained layer  $Si_{1-x}Ge_x$  undulator crystal*. Nucl. Instrum. Meth. B **309**, 37 (2013).
- [13] T. N. Tran Thi, J. Morse, D. Caliste, B. Fernandez, D. Eon, J. Härtwig, C. Barbay, C.

- Mer-Calfati, N. Tranchant, J. C. Arnault, T. A. Lafford, and J. Baruchel. *Synchrotron Bragg diffraction imaging characterization of synthetic diamond crystals for optical and electronic power device applications*. J. Appl. Cryst. **50**, 561 (2017).
- [14] B. G. de la Mata, A. Sanz-Hervás, M. G. Dowsett, M. Schwitters, and D. Twitchen. *Calibration of boron concentration in CVD single crystal diamond combining ultralow energy secondary ions mass spectrometry and high resolution X-ray diffraction*. Diamond and Rel. Mat. **16**, 809 (2007).
- [15] U. Uggerhøj. *The interaction of relativistic particles with strong crystalline fields*. Rev. Mod. Phys. **77**, 1131 (2005).
- [16] SLAC Site Office: *Preliminary Conceptual Design Report for the FACET-II Project at SLAC National Accelerator Laboratory*. Report SLAC-R-1067, SLAC (2015).
- [17] The corresponding values of the transverse beam size and divergence, used in the current simulations, are  $\sigma_{x,y} = 32, 10$  microns and  $\sigma_{\phi_{x,y}} = 10, 30$   $\mu$ rad.
- [18] A. V. Korol and A. V. Solov'yov. Crystal-based intensive gamma-ray light sources. *Europ. Phys. J. D* **74**, 201 (2020).